Colloid Polym Sci (2007) 285:641–647
DOI 10.1007/s00396-006-1606-4

ORIGINAL CONTRIBUTION

Peanut-shaped aggregation of $CaCO_3$ crystallites in the presence of an amphiphilic derivative of carboxymethylchitosan

Yaping Huang · Qiang Shen · Weiping Sui · Meili Guo · Ying Zhao · Dujin Wang · Duanfu Xu

Received: 22 July 2006 / Accepted: 5 October 2006 / Published online: 17 November 2006

Abstract An amphiphilic derivative of carboxymethylchitosan (CMCS), (2-hydroxyl-3-butoxyl)propyl-CMCS (HBP-CMCS), was used as an organic additive in the precipitation process of calcium carbonate ($CaCO_3$). HBP-CMCS molecules can interact with calcium ions, the functional groups of which act as active sites for the nucleation and crystallization of $CaCO_3$. Simultaneously, HBP-CMCS molecule also functionalizes as a colloidal stabilizer to prohibit the sedimentation of the grown $CaCO_3$ crystals, depending upon the molar ratio of the initial Ca^{2+} ions to the repeat units of HBP-CMCS molecules. The combination investigations of scanning electron microscopy, X-ray diffraction, and Fourier transform infrared spectroscopy on the precipitated $CaCO_3$ crystals proved that concentrations of HBP-CMCS and Ca^{2+} exert great influence on the crystallization habit of $CaCO_3$, such as the nucleation, growth, morphology, crystal form, etc. The formation of the peanut-shaped $CaCO_3$ particles suggests the template effect of HBP-CMCS molecules on the aggregation behavior of $CaCO_3$ nanocrystals.

Keywords Calcim carbonate · Crystallization · Chitosan derivative · Template effect · Peanut-shaped aggregates

Y. Huang · Q. Shen · Y. Zhao · D. Wang (✉) · D. Xu
State Key Laboratory of Polymer Physics and Chemistry,
Joint Laboratory of Polymer Science and Materials,
Institute of Chemistry, Chinese Academy of Sciences,
Beijing 100080, People's Republic of China
e-mail: djwang@iccas.ac.cn

Q. Shen
e-mail: qshen@sdu.edu.cn

Q. Shen
Key Laboratory for Colloid and Interface Chemistry
of Education Ministry, Shandong University,
Jinan 250100, People's Republic of China

Y. Huang · M. Guo
Department of Material Science and Engineering,
Beijing University of Aeronautics and Astronautics,
Beijing 100083, People's Republic of China

W. Sui
School of Chemistry and Chemical Engineering,
University of Jinan,
Jinan 250022, People's Republic of China

Introduction

It is well known that biominerals such as mollusk shells, teeth, and skeleton in organisms have superior performance to the unnatural compartment not only for the mechanical strength but also for the functional properties [1–4]. Among these biomaterials, the nacre of mollusk shell, one of the most often mentioned natural biomineralization materials, has a laminated structure composed of calcium carbonate ($CaCO_3$) crystals and biological macromolecules such as chitin and silk-fibroin-like protein [5]. In vivo research showed that chitin or protein plays an important role in the biomineralization [6, 7], and some of the included proteins were extracted, characterized, and used to mimic the process in vitro [8, 9]. The consequent crystallization of $CaCO_3$ showed that proteins extracted from an aragonitic shell layer induce the formation of amorphous $CaCO_3$ before its transformation into the aragonitic crystal formation, and proteins extracted from calcitic shell layers induce mainly calcite formation [10]. Although protein components are well known to be responsible for the mineralization, it is also believed that, as an insoluble substrate, chitosan or chitin plays an important role in mineralization process [6, 11]. Up to now, a series of water-soluble

derivatives of chitosan or chitin have been prepared and applied for the mimetic investigation on the process of biomineralization, and some interesting results have been obtained to explain the biomineralization mechanisms [12].

In the previous work [13–15], we prepared and characterized carboxymethylchitosan (CMCS) and (2-hydroxyl-3-butoxyl)propyl-carboxymethylchitosan (HBP-CMCS). When CMCS was used as an organic additive in the precipitation process of $CaCO_3$, Fourier transform infrared (FTIR) spectra proved that there is a strong electrostatic interaction between the CMCS functional groups and calcium ions. Even at pH ~7, CMCS could react with calcium ions in aqueous solutions, resulting in opaque dispersions [13, 14]. In the Kitano solutions for the crystallization of $CaCO_3$, CMCS at the concentration of 100 ppm could generate the shuttlecock aggregates due to the existence of both the template effect of CO_2 bubbles and the $CaCO_3$ nanocrystals temporarily stabilized by the organic additives. At the meantime, the bridge effect of CMCS molecules caused the spherical nanocrystals to aggregate into irregular wires when the CMCS concentration was lower than 5,000 ppm. The synergistic adduct between the shuttlecocks and the wires shows the petunia-shaped superstructure of $CaCO_3$ [14]. When CMCS molecules were hydrophobically modified, the resulted HBP-CMCS was demonstrated to possess surface activity and to form aggregates by the hydrophobic association [15]. Although its critical aggregation concentration (ca. 20 g/l) is too high to be widely used as an organic additive in the template synthesis of inorganic minerals, HBP-CMCS molecule is also believed to play an important role in the crystallization and aggregation processes of $CaCO_3$. The purpose of the present paper was to investigate the crystallization habit of $CaCO_3$ in the presence of HBP-CMCS and the formation mechanism of peanut-shaped $CaCO_3$ aggregate. Moreover, this is expected to explore the possible enrichment of metal ion mechanism on organic matrices and further to understand the in vivo biomineralization mechanism.

Materials and methods

Materials

HBP-CMCS was prepared (Scheme 1), and the substituted degree of carboxymethyl was 0.8 and the substituted degree of *N*-(2-hydroxyl-3-butoxyl) propyl was 0.2 [15]. Calcium chloride dihydrate (Sigma-Aldrich, 99+%) and sodium carbonate anhydrous (Tianjin Fuchen Chemical Plant) were used without further purification. Doubly deionized water was used to prepare aqueous solutions of $CaCl_2$, Na_2CO_3, and HBP-CMCS just before use.

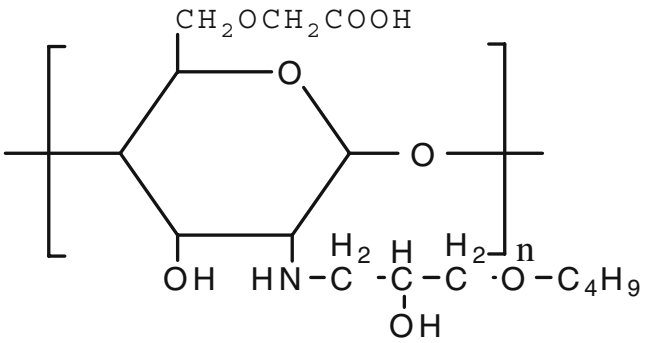

Scheme 1 The chemical structure of HBP-CMCS

$CaCO_3$ synthesis

$CaCO_3$ crystals were precipitated by pouring 50 ml of 0.05 M Na_2CO_3 solution into 50 ml of HBP-CMCS solution and then by adding equimolar amount of $CaCl_2$ solution (100 ml). The mixture was continuously stirred at a constant rate of 200 rpm by a Teflon-coated magnetic stirring bar to minimize the heterogeneous nucleation at the glass wall. The crystallization process was subsequently continued for 10 h to allow further crystal growth by Ostwald ripening. The reaction vessel was kept at 25±1 °C in a thermostatic bath. The precipitated $CaCO_3$ crystals were filtered, rinsed with deionized water, and dried at 35 °C overnight for further measurements.

Characterization of $CaCO_3$ crystals

All samples were Pt-coated before they were examined by a Hitachi S-4300 scanning electron microscope (SEM), fitted with a field emission source, and operated at an accelerating voltage of 15 kV. The X-ray diffraction (XRD) measurements were conducted by using a Rigaku D/max-2400 powder X-ray diffractometer with Cu Kα radiation (40 kV, 120 mA), and 0.02° step and 2θ range of 20–60° were selected to analyze the crystal polymorphism. FTIR spectroscopic measurements were performed on a Bruker EQUINOX 55 spectrometer with 32 scans and 4 cm^{-1} resolution. Particle size and the size distribution for the obtained $CaCO_3$ crystals were calculated by using an image analysis program (Scion Image—PC version). The organic content in the prepared $CaCO_3$ crystals was tested by thermogravimetric analysis (TGA) using a Perkin-Elmer TGA-7m, purged with nitrogen gas.

Results and discussion

The interaction between HBP-CMCS and calcium ions

In the concentration range of 50–2,000 ppm, the pH values of the aqueous HBP-CMCS solutions kept almost constant

(~8.8), the addition of 0.05 M Na_2CO_3 caused the pH value rising up to ~11.0, then the addition of equimolar amount of $CaCl_2$ decreased the pH value to ~10.0. After that, the pH value of the precipitation reaction system decreased gradually with the increase of incubation time until it reached a constant of ~9.0. It has been reported that, in the absence of Na_2CO_3, another format of the modified CMCS molecules can react with $CaCl_2$ (*aq.*) due to the electrostatic interaction and resulting in opaque dispersions [14]. This suggests that precipitation of $CaCO_3$ and Ca_x^{2+} (HBP-CMCS) may simultaneously occur in the mixture of $CaCl_2$/HBP-CMCS/Na_2CO_3. The two processes are described as follows:

$$Ca^{2+}(\text{aq.}) + CO_3^{2-}(\text{aq.}) \leftrightarrow CaCO_3(s) \quad (1)$$

$$xCa^{2+}(\text{aq.}) + HBP - CMCS(\text{aq.}) \leftrightarrow Ca_x^{2+}(HBP - OCMCS)(s) \quad (2)$$

In the process of $CaCO_3$ particle incubation, the initially formed amorphous $CaCO_3$ will transfer into various crystalline forms depending upon the experimental conditions (i.e., temperature, pH, stirring, property and concentration of organic additives, etc.) [16]. This means that: the first equation slowly moves right to produce crystalline particles; at the meantime, the Ca_x(HBP-CMCS) precipitates will be reverted to water-soluble HBP-CMCS and Ca^{2+}. The decrease of the active concentration of Ca^{2+} ions causes the decreases of the carbonate ions and the pH value of the precipitation system. Thus, after the complete precipitation of $CaCO_3$, the resulted dispersions should be clear. In fact, the active sites of carboxyl group in each glucose unit (Scheme 1) could induce the heterogeneous nucleation of $CaCO_3$, and the consequent crystallization and aggregation of $CaCO_3$ could be modulated by the bridging effect of HBP-CMCS molecules to produce chain-like floccules (Fig. 1a and the inset). If these floccules were completely rinsed out of water, the peanut-shaped aggregates of $CaCO_3$ crystals in nanosized scale can clearly be observed (Fig. 1b). The experimental results also showed that, at low molar ratio of calcium ion to the repeat unit of HBP-CMCS, it was very difficult for $CaCO_3$ to precipitate. Under this condition, HBP-CMCS molecules first serve as the active sites for the heterogeneous nucleation of $CaCO_3$ and then functionalize as colloidal stabilizer for the growing of $CaCO_3$ particles.

Effect of HBP-CMCS concentration on the crystal morphology

From the Eq. 1 listed above, it can be imagined that the higher concentration of HBP-CMCS, the smaller x value of calcium ions, coordinated with each polymer molecules. In other words, the higher HBP-CMCS concentration, the smaller fraction of polymer molecules, was initially contaminated by calcium ions to produce the organic precipitate of Ca_x(HBP-CMCS). In fact, the enrichment of Ca^{2+} ions at the negatively charged surface of polymers partly simulates the in vivo biomineralization in organisms. Then, the HBP-CMCS molecules could provide the nucleation sites for the crystallization of $CaCO_3$ and functionalize as stabilizing agent for colloidal particles, depending upon the molar ratio of Ca^{2+} ion to the repeat unit of HBP-CMCS molecule. When the concentration of Ca^{2+} ions was fixed at 2.50×10^{-2} M, the presence of different concentration of HBP-CMCS resulted in different characteristics of $CaCO_3$ crystals shown in Figs. 2 and 3.

At the same experimental condition, $CaCO_3$ crystallization in the absence of polymers only resulted in the typical rhombohedral calcite [16], which is shown in the inset of Fig. 2a. The addition of 100 ppm HBP-CMCS, however, greatly changed the morphology of precipitated $CaCO_3$ crystals (Fig. 2a), and the corresponding XRD pattern showed the polymorphic nature of calcite and vaterite (Fig. 3a-A). After being calcined at 600 °C for several hours, these $CaCO_3$ particles were proved to be the mixture of rhombohedrons and spheres, suggesting the prohibition effect of HBP-CMCS on the transformation of vaterite to calcite. From Fig. 3(a-A), it is also easy to estimate, according to Rao's equation [17], 38.8 wt% of vaterite that exists in the polycrystalline mixture. When HBP-CMCS

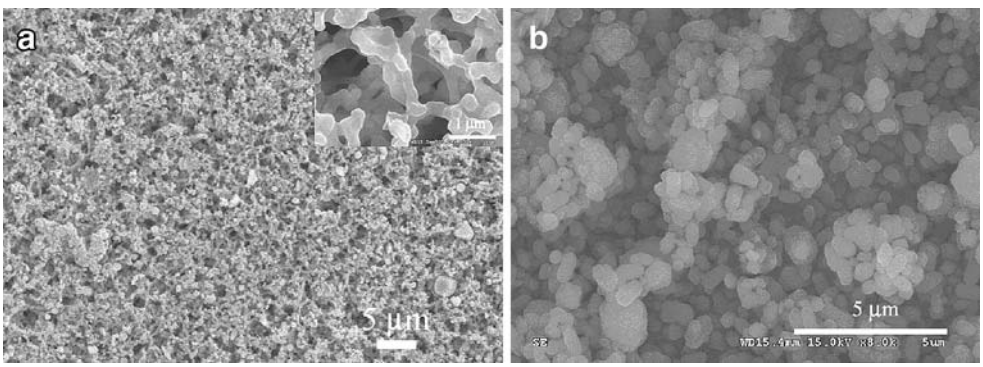

Fig. 1 SEM images of the floccules (**a**) and $CaCO_3$ crystals (**b**) obtained from 100 ppm aqueous HBP-CMCS solution with the initial concentration of Ca^{2+} ions at 6.25×10^{-3} M. *Inset* in (**a**) is the magnified SEM picture of the floccules

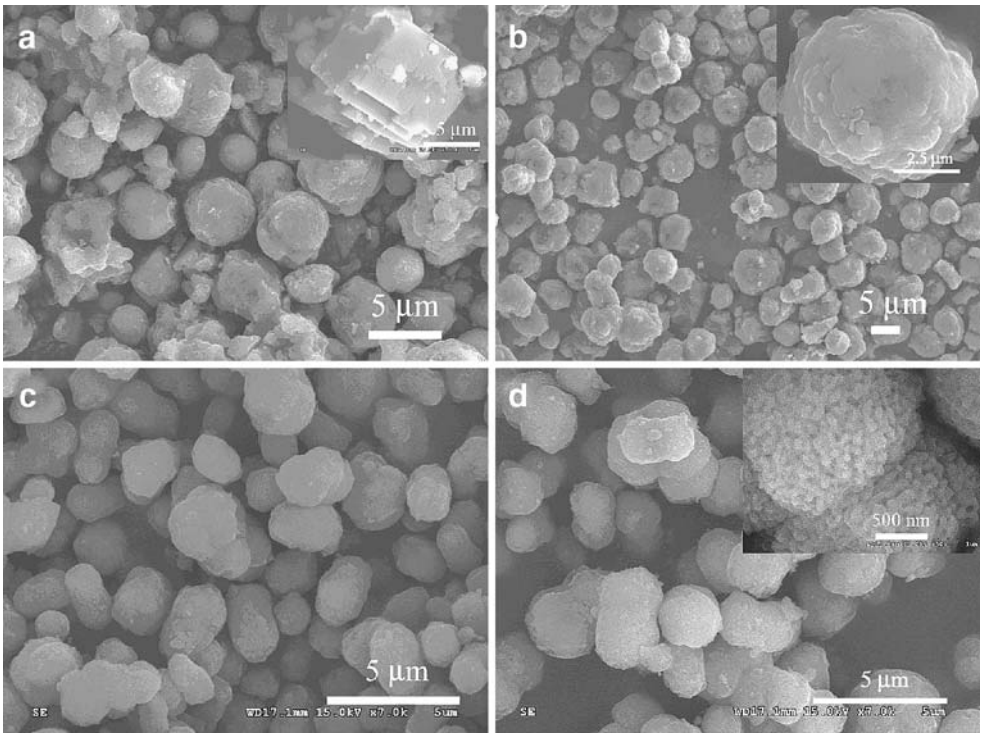

Fig. 2 SEM images of the $CaCO_3$ crystals precipitated from aqueous solutions in the presence of 100 (**a**), 500 (**b**), 1,000 (**c**), and 2,000 ppm (**d**) HBP-CMCS, respectively. *Inset* in (**a**) shows the typical morphology of the $CaCO_3$ crystal obtained in the absence of organic additives. *Inset* in (**b**) is the magnified SEM picture of a selected $CaCO_3$ particle. *Inset* in (**d**) shows the SEM picture of the peanut-shaped aggregate of calcite calcined at ~600 °C for several hours

concentration increased to 500 ppm, the resulted $CaCO_3$ crystals also showed the irregular morphology, possibly due to the incomplete rinse of HBP-CMCS molecules (Fig. 2b). Fig. 3a-B exhibits the same XRD characteristics as Fig. 3a-A, indicating 21.2 wt% of vaterite. The inset in Fig. 2b clearly shows that the organic additives absorbed on the surface of $CaCO_3$ particles are difficult to be completely washed away in centrifugation process.

In the presence of 1,000 ppm HBP-CMCS, the rapid mixing of equal volume of $CaCl_2$ (2.5×10^{-2} M) and Na_2CO_3 (2.5×10^{-2} M) solutions resulted in peanut-shaped $CaCO_3$ particles (Fig. 2c). In addition, the corresponding XRD spectrum (Fig. 3a-C) coincides with that of the calcite particles sampled in the absence of organic additives, indicating that the peanut-shaped particles are the thermodynamically stable calcite. While in the presence of 2,000 ppm HBP-CMCS, the obtained calcite particles (Figs. 2d and 3a-D) also showed the same crystal morphology and habit as these are shown in Figs. 2c and 3a-C. It is surprising that, even at a high concentration of 2.5×10^5 ppm, the presence of HBP-CMCS molecules also resulted in the peanut-shaped aggregates of calcite. Although it is difficult to find the absorption film of HBP-CMCS molecules on the surface of $CaCO_3$ aggregates from Fig. 2c,d, the inset in Fig. 2d shows the "porous" morphology after the calcination of organic substances. The organic additives absorbed on crystal surfaces and/or embedded in $CaCO_3$ particles can be detected by TGA analyses, which are shown in Fig. 3b. From Fig. 3b, it can be seen that, for the $CaCO_3$ particles obtained in the

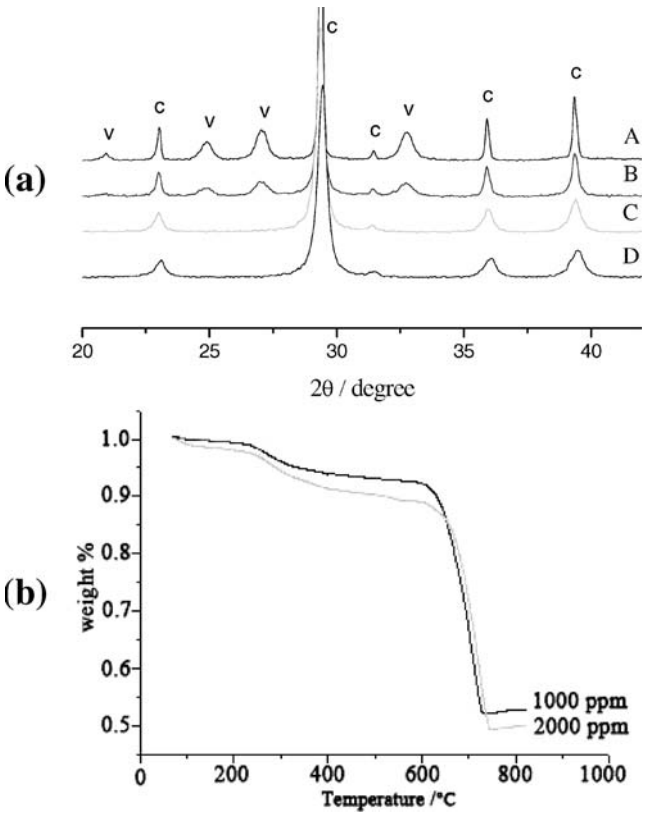

Fig. 3 **a** XRD results of the $CaCO_3$ crystals obtained from aqueous solutions of 100 (*A*), 500 (*B*), 1,000 (*C*), and 2,000 ppm (*D*) HBP-CMCS, respectively. The *marked symbol c* represents calcite corresponding to *hkl*: 012, 104, 006, 110, and 113, respectively; and the *letter v* denotes vaterite corresponding to *hkl*: 004, 110, 112, and 114, respectively. **b** TGA results of the $CaCO_3$ crystals shown in Fig. 2c, d

presence of 1,000 and 2,000 ppm HBP-CMCS, each TGA measurement shows two decomposing processes. The first decomposing onset at ca. 220 °C corresponds to the carbonization of HBP-CMCS molecules, and the second one at ca. 620 °C corresponds to the decomposition of $CaCO_3$ crystals. The weight loss during the first decomposition course is ca. 4.0 or 5.0% in the presence of 1,000 or 2,000 ppm HBP-CMCS, respectively, while the residual mass (i.e., only the $CaCO_3$ crystals) was determined to have a weight loss of ca. 40%. Therefore, Fig. 3b further proves that HBP-CMCS molecules are chemically interacted and/or absorbed on the surfaces of the precipitated $CaCO_3$ crystals.

So far as the particle size and size distribution are concerned, when the concentration of calcium ions was fixed at 2.50×10^{-2} M, the average particle sizes sampled in the presence of 100, 500, 1,000, and 2,000 ppm HBP-CMCS are 5.1±1.5 μm (Fig. 2a), 7.5±1.0 μm (Fig. 2b), 2.2±0.5 μm (Fig. 2c), and 2.1±0.5 μm (Fig. 2d), respectively. This indicates that, in the HBP-CMCS dispersions containing a fixed concentration of calcium ions, the heterogeneous nucleation functionalized for the crystallization of $CaCO_3$, depending upon the concentration of HBP-CMCS.

From Fig. 3a, it is also noticeable that the full width at half height of each XRD peak decreases with the increase of HBP-CMCS concentration. For example, the full width at half height for the (110) peak of calcite gradually changes from 0.18° (100 ppm HBP-CMCS) to 0.53° (2000 ppm HBP-CMCS). According to the Scherrer equation [18], the average size of $CaCO_3$ particles decreases with the gradually broadening nature of XRD peaks, further proving that the higher the HBP-CMCS concentration, the smaller the average particle size there is for $CaCO_3$ crystals or their aggregates.

Effect of the initial concentration of calcium ion

When the HBP-CMCS concentration was fixed at 100 ppm, the initially different concentration of Ca^{2+} ions was used to test the above crystallization phenomena. Figure 4 shows the FTIR spectra for the $CaCO_3$ precipitated from the initially different concentration of Ca^{2+} ions. In Fig. 4, the FTIR absorption peaks at 712 and 745 cm^{-1} are assigned to the characteristic absorption bands of calcite and vaterite, respectively [19, 20]. Although the molar ratio of Ca^{2+} ion to the repeat unit of HBP-CMCS molecule varied in the range of 4–30, the low concentration of HBP-CMCS always resulted in the polycrystalline particles of calcite and vaterite. Under this circumstance, vaterite content decreased with the decreasing molar ratio of Ca^{2+} ion to the repeat unit of HBP-CMCS molecule, coinciding with the results shown in Fig. 3a.

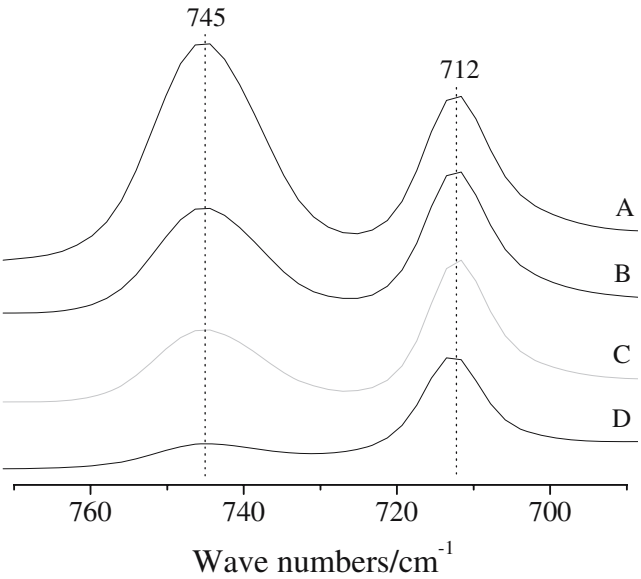

Fig. 4 FTIR spectra of $CaCO_3$ precipitated from 100 ppm HBP-CMCS solution after rapid mixing of $CaCl_2$ with equimolar amount of Na_2CO_3. The initial concentrations of Ca^{2+} ions were 2.5×10^{-2} (*A*), 1.25×10^{-2} (*B*), 6.25×10^{-3} (*C*), and 1.25×10^{-3} M (*D*), respectively

It seems that the initial concentration of Ca^{2+} ion has the same morphological effect on $CaCO_3$ crystals. For example, at high molar ratio of Ca^{2+} ion to HBP-CMCS, the obtained precipitates have the same irregular morphologies as these are shown in Fig. 2a,b, while at the relatively low molar ratio of ca. 8, the peanut-shaped aggregates of polycrystalline $CaCO_3$, with the average size of 1.4±0.2 μm, are shown in Fig. 5a. However, the rapid mixing of 1.25×10^{-3} M $CaCl_2$ with equimolar amount of Na_2CO_3 resulted in spherical polycrystalline $CaCO_3$ with the average size of 350±50 nm (Fig. 5b). It is supposed that, at low concentration of Ca^{2+} ions, the relatively low salt effect caused HBP-CMCS backbones to stretch. Then, the distance between the adjacent functional groups on the organic backbone is relatively big. Consequently, the formed $CaCO_3$ spheres are too far away to aggregate, which means that both HBP-CMCS and initial Ca^{2+} ion concentrations are very important for the formation of the peanut-shaped aggregates of $CaCO_3$. From Fig. 5, it can easily be seen that the size of the obtained $CaCO_3$ crystals is nanoscaled, and the particle size decreases with the decrease of Ca^{2+} concentration. At the extremely low concentration of Ca^{2+} ions, the nucleation sites provided by 100 ppm HBP-CMCS are so many that it only favors the formation of nanocrystals.

Morphological effect of stirring on $CaCO_3$ aggregates

After pouring the 2.50×10^{-2}-M $CaCl_2$ solution into the mixture of HBP-CMCS/Na_2CO_3 (2.5×10^{-2} M), the precipitation system was stirred for 1 min. Then, the incubation

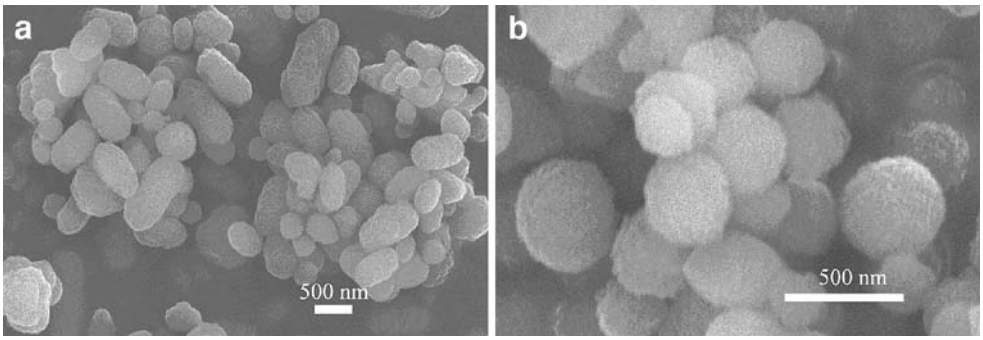

Fig. 5 SEM images of $CaCO_3$ precipitated from 100 ppm HBP-CMCS solution after rapid mixing of $CaCl_2$ with equimolar amount of Na_2CO_3. The initial concentrations of Ca^{2+} ions were fixed at 6.25×10^{-3} (**a**) and 1.25×10^{-3} M (**b**), respectively

system was kept still to investigate the effect of stirring on the crystallization and aggregation behavior of $CaCO_3$. FTIR measurements showed the same polymorphic evolvement against HBP-CMCS concentration as that shown in Fig. 3a. When HBP-CMCS concentration was fixed at 100 ppm, the morphology of the resulted polycrystalline particles (i.e., vaterite and calcite) was shown in Fig. 6a. This is almost the same as that shown in Fig. 2a. The presence of 500 ppm HBP-CMCS resulted in spherical aggregates of polycrystalline particles with irregular morphology, with parts of the particles showing peanut-shaped superstructure (Fig. 6b). At high HBP-CMCS concentrations, the morphologies of the obtained $CaCO_3$ that was incubated under still condition were shown in Fig. 6c,d, also exhibiting peanut-shaped superstructures.

From Fig. 6a,d, it can be seen that the precipitated peanut-shaped superstructures in the presence of 100 ppm HBP-CMCS have rough surfaces, while those in the presence of 2,000 ppm HBP-CMCS have relatively smooth surfaces. This also coincides with the results of Fig. 3a showing that the higher the concentration of HBP-CMCS, the smaller the particle size of $CaCO_3$ crystals. The comparison of Fig. 6 with Fig. 2 suggests an interesting effect of stirring on the aspect ratio of peanut-shaped aggregates. Without stirring, the supplement of the local Ca^{2+} concentration around $CaCO_3$ nuclei is relatively slow, resulting in the relatively low aspect ratio of particle aggregates with low surface energy. This more or less coincides with the growth of $CaCO_3$ nuclei at the low concentration of calcium ion shown in Fig. 5b.

Conclusions

We have shown in this study that HBP-CMCS has remarkable influence on the crystallization habit of $CaCO_3$

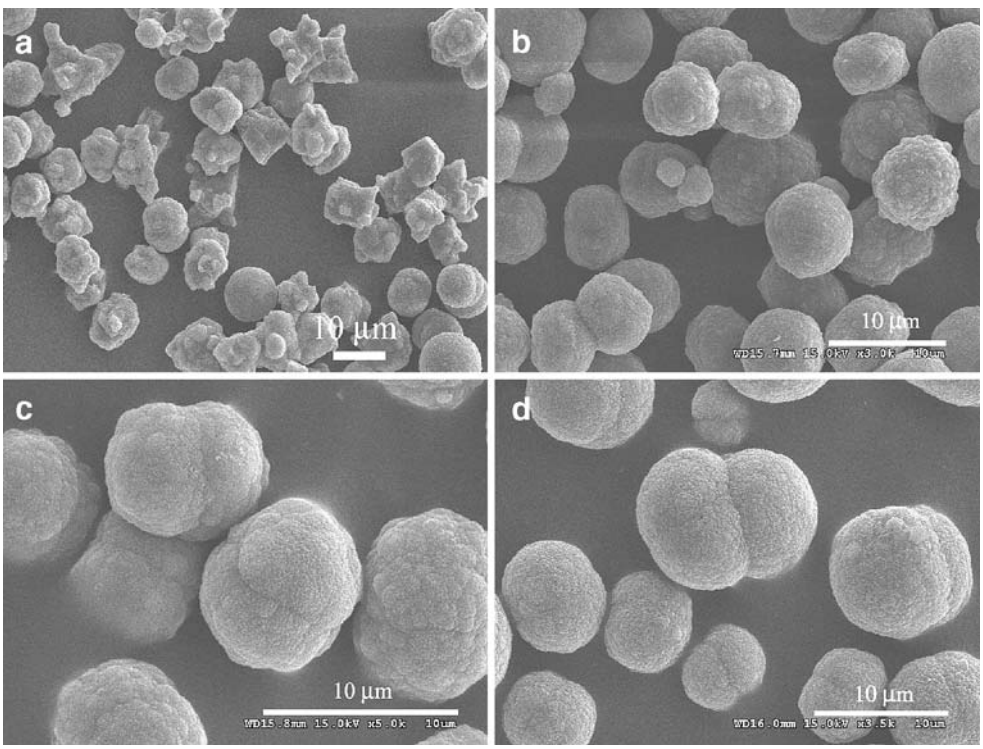

Fig. 6 SEM images of the $CaCO_3$ crystals precipitated from aqueous solutions in the presence of 100 (**a**), 500 (**b**), 1,000 (**c**), and 2,000 ppm (**d**) HBP-CMCS, respectively. After pouring 2.5×10^{-2} M $CaCl_2$ solution into the mixture of HBP-CMCS/Na_2CO_3 (2.5×10^{-2} M), the precipitation system was stirred for 1 min and consequently kept still during the whole incubation time

due to the strong electrostatic interaction between Ca^{2+} ions and carboxyl groups and the dispersion capability of the investigated polymer for inorganic particles. The crystal size and form of $CaCO_3$ gradually change with the concentration variation of both HBP-CMCS and Ca^{2+} ions. The present results underline a new strategy for the biomimetic synthesis of the $CaCO_3$ superstructure by the self-assembly of mesoscale crystals in a simple way, suggesting a convenient method to investigate morphological effect of biomolecules on the biomineralization of $CaCO_3$ in vivo.

Acknowledgements The financial supports from the National Natural Science Foundation of China (20471064) and the Natural Science Foundation of Shandong Province (Y2004B05) are gratefully acknowledged.

References

1. Curry JD, Talor JD (1974) J Zool 173:395
2. Curry JD, Kohn AJ (1976) J Mater Sci 11:1615
3. Curry JD (1979) J Zool 188:301
4. Muzzarelli C, Muzzarelli RAA (2002) J Inorg Biochem 92:89
5. Sellinger A, Weiss PM, Nguyen A, Lu YF, Assink RA, Gong WL, Brinker CJ (1998) Nature 394:256
6. Falini G, Weiner S, Addadi L (2003) Calcif Tissue Int 72:548
7. Mikkelsen A, Engelsen SB, Hansen HCB, Larsen O, Skibsted LH (1997) J Cryst Growth 177:125
8. Ishii K, Tsutsui N, Watanabe T, Yanagisawa T, Nagasawa H (1998) Biosci Biotechnol Biochem 62:291
9. Blank S, Arnoldi M, Khoshnavaz S, Treccani L, Kuntz M, Mann K, Grathwohl G, Fritz M (2003) J Microsc 212:280
10. Levi Y, Albeck S, Brack A, Weiner S, Addadi L (1998) Chem Eur J 4:389
11. Zhang SK, Gonsalves KE (1998) Langmuir 14:6761
12. Zhang SK, Gonsalves KE (1995) Mater Sci Eng C 3:117
13. Liang P, Shen Q, Zhao Y, Zhou Y, Wei H, Lieberwirth I, Huang YP, Wang DJ, Xu DF (2004) Langmuir 20:10444
14. Liang P, Zhao Y, Shen Q, Wang DJ, Xu DF (2004) J Cryst Growth 261:571
15. Sui WP, Wang SF, Chen GH, Xu GY (2004) Carbohydr Res 339:1113
16. Wei H, Shen Q, Zhao Y, Wang DJ, Xu DF (2003) J Cryst Growth 250:516
17. Rao MS (1973) Bull Chem Soc Jpn 46:1414
18. Hua RN, Zang CY, Shao C, Xie DM, Shi CS (2003) Nanotechnology 14:588
19. Shen Q, Wei H, Wang LC, Zhou Y, Zhao Y, Zhang ZQ, Wang DJ, Xu GY, Xu DF (2005) J Phys Chem 109:18342
20. Dupont L, Portemer F, Figlarz M (1997) J Mater Chem 7:797